The 2016 World Congress on
Advances in Civil, Environmental, and Materials Research (ACEM16)
Jeju Island, Korea, August 28-September 1, 2016

Structural and Magnetic Properties of Monodispersed Iron Oxide Nanoparticles for use in Magnetic Resonance Imaging

*Saira Riaz[1)], S Sajjad Hussain[2)] and Shahzad Naseem[3)]

[1), 2), 3)] *Centre of Excellence in Solid State Physics, University of the Punjab, Lahore, Pakistan*
[1)] saira.cssp@pu.edu.pk

ABSTRACT

During the last few years, magnetic nanoparticles (NPs) have attracted global attraction due to their impending biomedical application i.e. Magnetic Resonance Imaging (MRI). Nanoparticles, to be utilized for MRI, must exhibit superparamagnetic behavior with relatively high value of saturation magnetization. Among various materials of interest magnetite and maghemite Superparamagnetic Iron Oxide Nanoparticles (SPION) has gained attraction due to not only its biocompatibility but also because of its various advantages including enhanced proton relaxation that leads to increased contrast effect with smaller amount of SPION. Sol-gel method is used to synthesize SPION NPs using ammonia as gelation agent. Concentration of ammonia is varied as 3mM to 7mM. XRD results confirm the formation of γ-Fe_2O_3 phase with use of ammonia concentration as 3mM, 4mM, 6mM and 7mM. Whereas, ammonia concentration of 5mM results in phase transition to Fe_3O_4. SEM images show formation of NPs with size less than 40nm. As ammonia concentration is increased to 5mM reduction in grain size to 20nm is observed. This reduction in grain size and phase transition to Fe_3O_4 is accompanied by magnetic transition from ferromagnetic behavior to superparamagnetic behavior.

1. INTRODUCTION

To date stem cells, found in all organism, are extensively investigated in various therapies including degenerative and regenerative medicines, genetic diseases. Once these cells are delivered into the human body their tracking and monitoring is extremely crucial. Several methodologies have been employed for this purpose including BLI (Bio Luminescence Imaging), PET (Positron Emission Tomography), fluorescence imaging, MRI, PECT (Photon Emission Computed Tomography) etc. Among various techniques MRI offers the advantages of high resolution, rapid in vivo imaging and most importantly no ionizing radiations are used in this technique. However sensitivity of MRI technique is low in comparison to BLI and PECT. Therefore, developing MRI contrast agents with enhanced sensitivity and efficiency is extremely important (Li et al. 2013,

[1)] Professor

Alcantara et al. 2016, Neubergera et al. 2005).

Contrast agents for MRI are categorized as: 1) T_1 agents; 2) T_2 agents. T_1 agents change the longitudinal relaxation time of water protons. This results in increased conspicuousness of cells and results in intense positive signal in the images. T_2 agents bring changes in transverse relaxation time of water protons. These agents result in dark negative signal (Li et al. 2016). Materials used for T_1 contrast agents include paramagnetic lanthanide, complexes of gadolinium etc. Instead, iron oxide nanoparticles having superparamagnetic nature are used as MRI contrast agents because of their high biocompatibility and high sensitivity. The major factors that influence T_2 relaxation process are: 1) Size of nanoparticles; 2) Crystallinity of nanoparticles and 3) Composition of nanoparticles (Li et al. 2016).

Iron oxide exhibits two significant phases i.e. magnetite (Fe_3O_4) and maghemite (γ-Fe_2O_3). Fe_3O_4 crystallizes in inverse spinal structure. In this structure oxygen ions are closely arranged along with presence of both Fe^{2+} (ferrous) and Fe^{3+} (ferric) cations. Fe(II) cations set in octahedral points while Fe(III) cations are randomly distributed in between tetrahedral and octahedral points. Four oxygen anions surround Fe^{3+} ions in tetrahedral sites while Fe^{2+} are surrounded by six octahedral sites. Fe^{2+} (ferrous) and Fe^{3+} (ferric) ions can displace themselves between octahedral and tetrahedral sites (Patsula et al. 2016, Riaz et al. 2014a,b). Magnetite (Fe_3O_4, ferrous ferrite) shows strongest magnetism due to the presence of Fe^{2+} on octahedral sites. It becomes ferromagnetic at room temperature and paramagnetic at Curie temperature of 850K (577°C). Maghemite, a polymorph of ferromagnetic iron oxide, γ-Fe_2O_3 is used on large scale in magnetic storage devices, magnetic optical devices and biomedical applications. At ambient conditions maghemite is a transition state between magnetite Fe_3O_4 and hematite α-Fe_2O_3. Maghemite has structure similar to that of magnetite but it only differs due to vacancies in cationic sublattice which reduces symmetry. Maghemite does not have Fe^{2+} ions. Two-thirds of the lattice site is occupied by Fe (III) ions regularly and one-third is empty. Reduction in size of particle of maghemite reduces the degree of vacancy order and this order diminishes for particle size less than 20nm (Craik 1975, Akbar et al. 2014a,b, Akbar et al. 2015).

An important factor that is neglected during the synthesis of iron oxide nanoparticles is the concentration of the gelation agent used. To investigate the effect of concentration of gelation agent used in sol-gel synthesis we here report sol-gel synthesis of iron oxide nanoparticles. Ammonia was used as gelation agent and concentration of ammonia was varied as 3mM, 4mM, 5mM, 6mM and 7mM.

2. EXPERIMENTAL DETAILS

Iron nitrate was used as starting material, whereas water and ethylene glycol as solvent. Iron nitrate was mixed in deionized water and ethylene glycol and stirred on hotplate to obtain iron oxide sol. The pH of sol was set to 7.0 using ammonia as gelation agent. The concentration of ammonia was varied as 3mM, 4mM, 5mM, 6mM and 7mM. Sol was then further heat treated on hotplate to obtain iron oxide nanoparticles.

Iron oxide nanoparticles were analyzed using Bruker D8 Advance X-ray diffractometer (XRD) with CuKα (1.5406Å) radiations. Magnetic properties were studied by Lakeshore's 7407 vibrating sample magnetometer (VSM).

3. RESULTS AND DISCUSSION

Fig. 1 shows XRD patterns for iron oxide nanoparticles prepared using ammonia as gelation agent and variation in ammonia concentration as 3mM, 4mM, 5mM, 6mM and 7mM. Presence of diffraction peaks corresponding to (310), (311), (321), (421), (430), (511) and (440) planes indicated the formation of phase pure γ-Fe_2O_3. As ammonia concentration was increased to 5mM phase transition to Fe_3O_4 was observed.

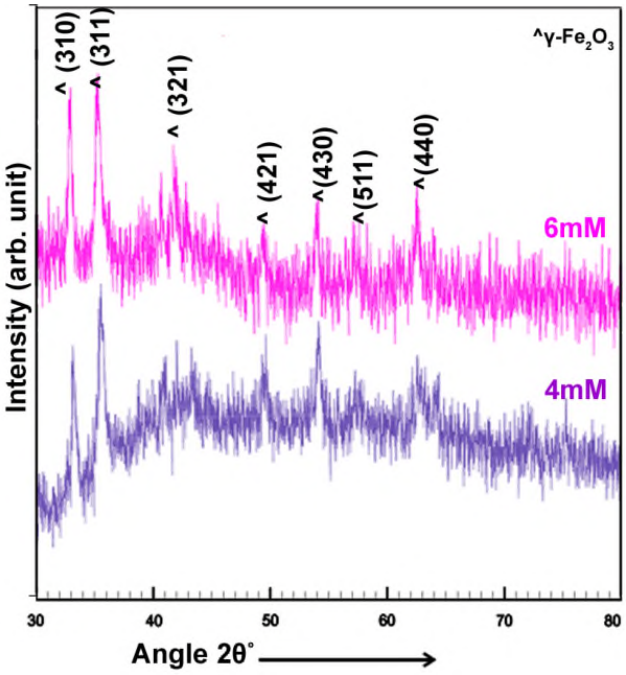

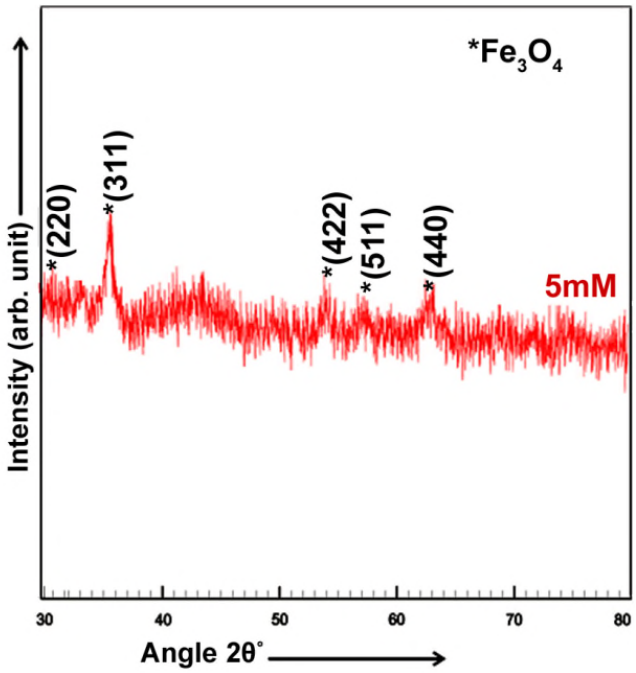

Fig. 1 XRD patterns for iron oxide thin films with ammonia concentration as 4mM, 5mM and 6mM

Fe_3O_4 and γ-Fe_2O_3 phases have similar crystallographic structure, the only difference is presence of vacancies at cationic sublattice in γ-Fe_2O_3 (Riaz et al. 2014a, Akbar et al. 2015). So, it becomes difficult to distinguish between the two phases on the basis of XRD patterns. However, careful analysis of JCPDS card nos. 72-4303 and 39-1346 reveal that there are some extraneous peaks present in γ-Fe_2O_3 that are not present in Fe_3O_4. Presence of diffraction peaks corresponding to planes (310) and (421) particularly indicate the formation of γ-Fe_2O_3. As ammonia concentration was further increased to 6mM and 7mM phase transition to γ-Fe_2O_3 was observed. This phase transition is associated with increase in number of OH^- ions with increase in ammonia concentration. Electron density gets disturbs due to protonation of OH^- groups. This results in electron entrapment and drop in valence from 2.5 to 2.0. Thus, the bond with the lattice gets broken and an electron from neighboring site jumps to compensate for the electron loss during the bond breaking process. Thus, the disturbance of whole lattice leads to phase transition from Fe_3O_4 and γ-Fe_2O_3 (Jolivet and Tronc 1988)

Crystallite size (*t*) (Cullity 1956), dislocation density (*δ*) (Kumar et al. 2011) and lattice parameters (Cullity 1956) were calculated using Eqs. 1-3

$$t = \frac{0.9\lambda}{B\cos\theta} \tag{1}$$

$$\delta = \frac{1}{t^2} \tag{2}$$

$$\sin^2\theta = \frac{\lambda^2}{4a^2}\left(h^2 + k^2 + l^2\right) \tag{3}$$

Crystallite size increases with increase in ammonia concentration up to 5mM. Further increase in ammonia concentration resulted in decrease in crystallite size and increase in dislocation density. Increase in crystallite size at low ammonia concentration is associated with increase in attractive forces between the particles. This leads to increase in crystallite size. However at high ammonia concentration phase transition from Fe_3O_4 to γ-Fe_2O_3 nanoparticles lead to decrease in crystallite size and increase in dislocation density. Lattice parameters and unit cell volume for iron oxide nanoparticles are plotted as a function of ammonia concentration in Fig. 3. Increase in lattice parameters and unit cell volume at ammonia concentration 5mM also indicates the formation of Fe_3O_4 phase as was observed in Fig. 1.

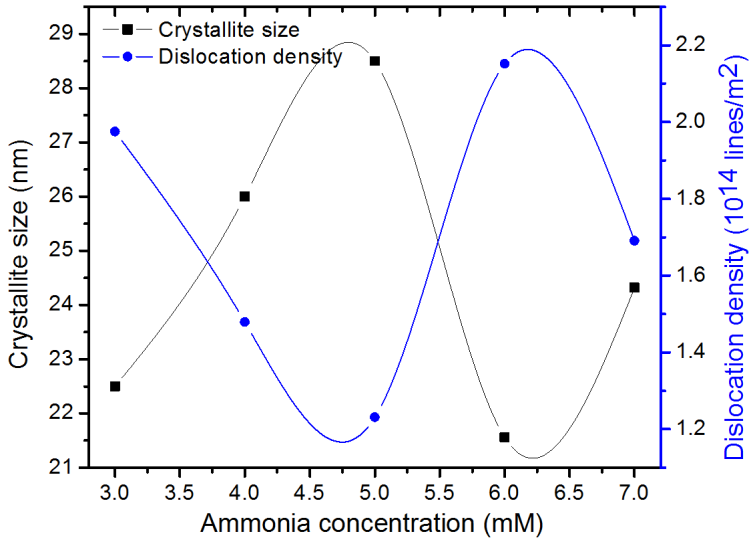

Fig. 2 Crystallite size and dislocation density plotted at various ammonia concentrations

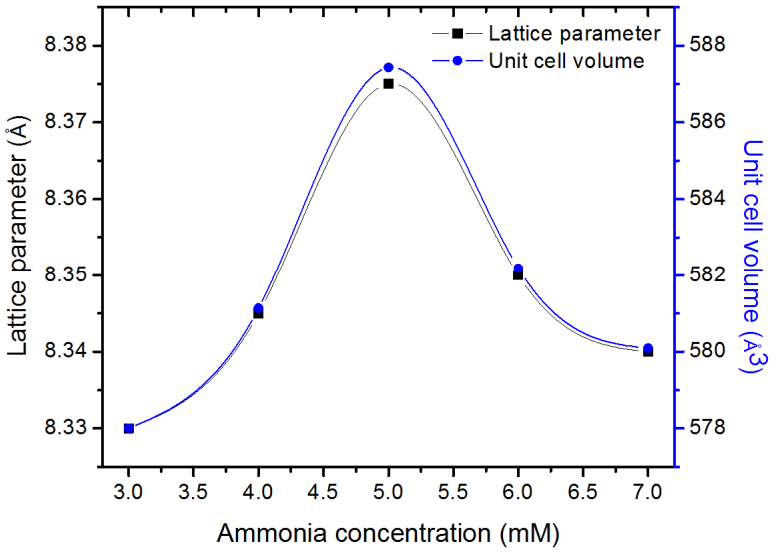

Fig. 3 Lattice parameters for iron oxide nanoparticles prepared with variation in ammonia concentration

Fig. 4 shows M-H curves for iron oxide nanoparticles. Nanoparticles prepared using ammonia concentration as 4mM resulted in ferromagnetic behavior. Transition to superparamagnetic behavior was observed for ammonia concentration 5mM. As ammonia concentration was further increased to 6mM transition from superparamagnetic behavior to ferromagnetic behavior was observed.

If the size of nanoparticles is small then thermal energy will be adequate to cause oscillation of the magnetization direction. This behavior is referred to as analogy between the large magnetic moment of nanosized particles and low magnetic moment of single paramagnetic atom. After removal of magnetic field the nanoparticles no longer exhibit magnetic interaction (Neuberger et al. 2005, Mahmoudi et al. 2015). This feature is important for its usability as MRI contrast agent. In addition, increase in saturation magnetization is also observed with increase in ammonia concentration to 5mM. This increase in saturation magnetization is indicative of phase transition from γ-Fe_2O_3 to Fe_3O_4.

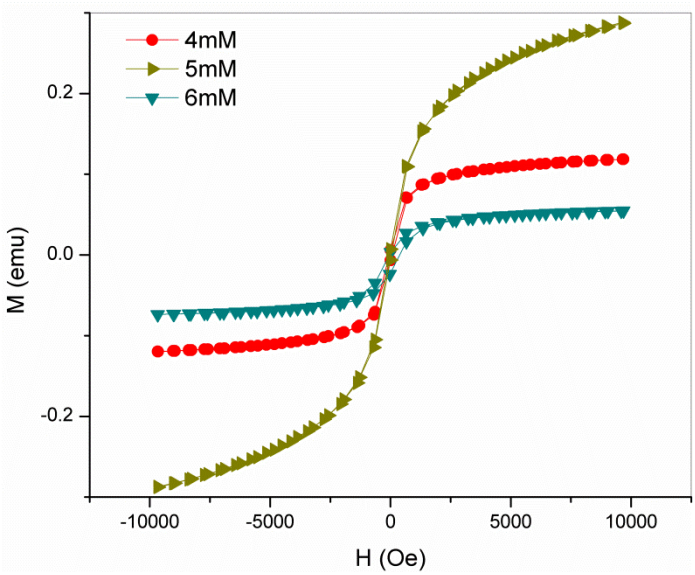

Fig. 4 M-H curves for iron oxide nanoparticles

4. CONCLUSIONS

Iron oxide nanoparticles were prepared using sol-gel method. During sol-gel synthesis ammonia was used as gelation agent and concentration of ammonia was varied as 3mM, 4mM, 5mM, 6mM and 7mM. XRD results confirmed the formation of Fe_3O_4 phase at ammonia concentration 5mM while 3-4mM and 6-mM resulted in formation of γ-Fe_2O_3 phase. Nanoparticles prepared using ammonia concentration 5mM resulted in superparamagnetic behavior with high saturation magnetization. While ferromagnetic behavior was observed for nanoparticles prepared using ammonia concentration as 3-4mM and 6-mM.

REFERENCES

Akbar, A., Riaz, S., Ashraf, R. and Naseem, S. (2014a), "Magnetic and magnetization properties of Co-doped Fe_2O_3 thin films," *IEEE Trans. Magn.*, **50**, 2201204

Akbar, A., Riaz, S., Ashraf, R. and Naseem, S. (2015), "Magnetic and magnetization properties of iron oxide thin films by microwave assisted sol–gel route," *J. Sol-Gel Sci. Technol.*, **74**,320–328.

Akbar, A., Riaz, S., Bashir, M. and Naseem, S. (2014b), "Effect of Fe^{3+}/Fe^{2+} Ratio on Superparamagnetic Behavior of Spin Coated Iron Oxide Thin Films," *IEE Trans. Magn.*, **50**, 2200804.

Alcantara, D.,Lopez, S., Martin, M.L.G. and Pozo, D. (2016), "Iron oxide nanoparticles as magnetic relaxation switching (MRSw) sensors: Current applications invnanomedicine," Nanomed.: Nanotechnol. Bio Med., **12**, 1253-1262

Craik, D. J. (1975), "Magnetic Oxides", New York: Wiley.

Cullity, B.D. (1956), "Elements of x-ray diffraction," Addison Wesley Publishing Company, USA.

Jolivet, J.P. and Tronc, E. (1988), "Interfacial electron transfer in colloidal spinel iron oxide, Conversion of Fe_3O_4-γFe_2O_3 in aqueous medium," *J. Colloid Inter. Sci*., **125,** 688-701

Kumar, N., Sharma, V., Parihar, U., Sachdeva, R., Padha, N. and Panchal, C.J. (2011) "Structure, optical and electrical characterization of tin selenide thin films deposited at room temperature using thermal evaporation method," *J. Nano- Electron. Phys.*, **3**, 117-126

Li, L., Jiang, W., Luo, K., Song, H., Lan, F., Wu, Y. and Gu, Z. (2013), "Superparamagnetic Iron Oxide Nanoparticles as MRI contrast agents for Non-invasive Stem Cell Labeling and Tracking," *Theranostics*, 3(8), 595-615

Mahmoudi, M., Sant, S., Wang, B., Laurent, S. and Sen, T. (2011), "Superparamagnetic iron oxide nanoparticles (SPIONs): Development, surface modification and applications in chemotherapy," *Adv. Drug Delivery Rev.*, **63**, 24–46

Neubergera, T., Schopfa, B., Hofmann, H., Hofmann, M. and Rechenberg, B. (2005), "Superparamagnetic nanoparticles for biomedical applications: Possibilities and limitations of a new drug delivery system," *J. Magn. Magn. Mater.*, **293**, 483–496

Patsula, V., Moskvin, M., Dutz, S. and Horak, D. (2016), "Size-dependent magnetic properties of iron oxide nanoparticles," J. Phys. Chem. Solid., **88,** 24–30.

Riaz, S., Akbar, A. and Naseem, S. (2014b), "Ferromagnetic Effects in Cr-Doped Fe_2O_3 Thin Films," *IEEE Trans. Magn.*, **50**, 2200704

Riaz, S., Ashraf, R., Akbar, A. and Naseem, S. (2014a), "Microwave Assisted Iron Oxide Nanoparticles—Structural and Magnetic Properties," *IEEE Trans. Magn.*, **50**, 2201504